Highly ordered monodomain ionic self-assembled liquid-crystalline materials

Y. Zakrevskyy,[1] B. Smarsly,[2] J. Stumpe,[1] and C. F. J. Faul[2,*]
[1]*Fraunhofer Institute for Applied Polymer Research, Science Campus Golm, Geiselbergstrasse 69, D-14476 Potsdam, Germany*
[2]*Max Planck Institute of Colloids and Interfaces, Research Campus Golm, Am Mühlenberg 1, D-14476 Potsdam, Germany*
(Received 19 August 2004; published 4 February 2005)

Liquid-crystalline properties of the ionic self assembled complex benzenehexacarboxylic-(didodecyltrimethylammonium)$_6$[BHC-(C_{12}D)$_6$] were investigated by polarizing microscopy, differential scanning calorimetry (DSC), x-ray analysis, null ellipsometry, UV and IR spectroscopy. The complex exhibits a bilayer smectic Sm-A_2 liquid-crystalline phase and aligns spontaneously. Alignment properties do not depend on the hydrophobic or hydrophilic treatment of the surfaces. The aligned complex possesses a negative ($\Delta n = -0.02$) homeotropically oriented optical axis, with layers aligned parallel to the surface. X-ray analysis of the aligned sample revealed a lamellar structure with a d spacing of 3.15 nm, consisting of sublayers of thicknesses $d_1 = 1.41$ and $d_2 = 1.74$ nm. This was confirmed by simple geometrical calculations and detailed temperature-dependent investigations, revealing that the first layer contains the BHC molecules and oppositely charged groups of the surfactants, and the second the alkyl tails of the surfactant. Changes in the order parameters (as calculated from the IR investigations) are correlated with the phase transitions as found by DSC. The properties of the complex are strongly influenced by the ionic interactions within the complex. The presence of these groups slows down the dynamics within the material sufficiently to allow for crystallization of the complex from an aligned LC phase into a single crystal domain, as well as restricting the transition to the isotropic phase.

DOI: 10.1103/PhysRevE.71.021701 PACS number(s): 61.30.Eb, 61.30.Gd

I. INTRODUCTION

The generation of low molecular weight thermotropic liquid-crystalline (LC) phases is highly dependent on the use of anisotropic molecular structures. This concept is already firmly established in literature [1]. The classical way to achieve this is to use elongated (rod- and lathlike) molecules. This type of molecules forms nematic and smectic LC phases. Some other nematic and most columnar phases are often made of disklike molecules [2]. The clear dependence of the mesomorphic properties on the geometrical shape of the molecules and on the combination of repulsive and attractive interactions of the van der Waals type has allowed the derivation of satisfactory models for describing LC systems theoretically [3]. In compounds containing strongly polar groups (e.g., $-CN$, $-NO_2$) the interaction of permanent and induced electrical dipoles plays a remarkable role in phase formation [4]. The reduced symmetry of molecules, that imparts form chirality, leads to a variety of interesting phases that are manifested in the formation of helical ordering of the constituent mesogens [5].

Further modifications and complications of the shape of the molecules lead to a variety of different LC phases; to this class belong nonconventional LC materials: laterally substituted and swallow-tailed liquid crystals [6,7]; hybrid molecules with a long rodlike rigid core ending with two half-disk moieties [8]; liquid-crystalline dimers and oligomers [9]. Interesting properties and functions can be obtained by introducing specific (noncovalent) interactions between molecules. For example, metal-containing LCs, also known as metalomesogens [10–12], combine the physical properties exhibited by LCs with the variety and range of metal-based coordination chemistry due to the presence of one or more metals. Geometries and functions not easily found in organic chemistry can result from the coordinated metal species. Charge-transfer [13] and hydrogen-bonding interactions are further examples of specific interactions between molecules that influence and even induce the formation of LC phases. Investigations into hydrogen-bonded systems were stimulated since it is a key interaction in chemical and biological processes in nature. A wide variety of structures of molecular liquid-crystalline complexes have been prepared through intermolecular hydrogen bonds [14,15].

One interaction strategy that has largely been neglected for the construction of mesogens is that of ionic interactions. The formation of supramolecular complexes using ionic interactions, or so-called ionic self-assembly (ISA), was recently shown to be a viable route for the production of self-organizing nanostructured materials [16]. The basic concept of the ISA strategy is shown in Fig. 1. Here the surfactant tails act as internal solvent, similar to the covalently attached tails in classical LC materials. It could be disputed that ions

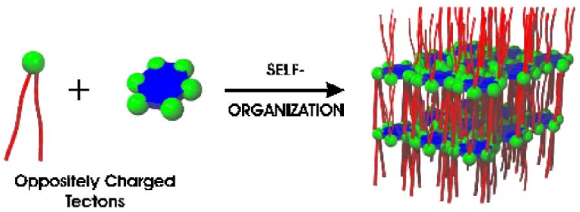

FIG. 1. (Color online) Ionic self-assembly (ISA) process.

*Corresponding author. Present address: School of Chemistry, Inorganic and Materials Chemistry, University of Bristol, BS8 1TS Bristol, UK. Email address: charl.faul@bristol.ac.uk

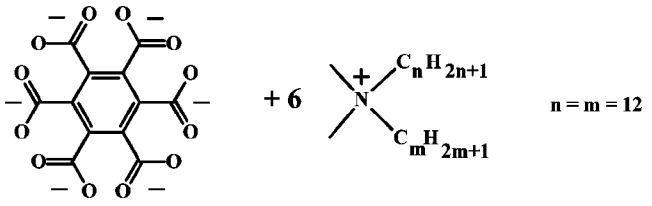

FIG. 2. Chemical structure of the BHC-$(C_{12}D)_6$ complex.

are responsible for the formation of lyotropic phases of surfactants and chromonic materials, and that the same is found in the ISA case. However, in the case of the ISA process the ions are used in the binding interaction within supramolecular self-assembly and replaces, for example, hydrogen bonds.

Liquid crystallinity was observed and reported for the first time for perylene-based ISA complexes [17]. The complexes show Schlieren-like textures and form columnar mesophases. In a proof-of-principle study (i.e., to show the potential for applications), different methods were tested to align of one of these LC complexes [18]. It was found that the materials properties have a large influence on the processability, and therefore the alignment, of such materials.

In order to investigate the influence of the ionic interactions on the formation of the LC phases, we start with a rather simple molecule with maximum symmetry. Benzene derivates have attracted some attention over the last few years as mesogens for the formation of a variety of columnar phases. Nuckolls *et al.* have investigated the use of crowded hexasubstituted benzene (more specifically alternatingly substituted with alkoxy and amide groups) in the formation of columnar structures in a series of papers [19–21]. They introduced the possibility for hydrogen bonding through the presence of amide groups, which provided further stabilization (in conjunction with π-π interactions). Müllen *et al.* [22] have shown that in the case where the central benzene of a hexaaryl-substituted system could be reduced to the hexaanion, a twisted central benzene molecule was produced in solution. Keeping furthermore in mind that the first (covalent) discotic systems were prepared from benzene-hexa-n-alkanoates in 1977 [23], we therefore selected mellitic acid/benzenehexacarboxylic acid (BHC) as tecton for this study. This tecton has the possibility to form a complex with six surfactant molecules, and can the covalent bonds between benzene ring and alkyl chains of the original discotic material now be replaced with ionic interactions. Didodecyldimethylammonium bromide ($C_{12}D$) was used as surfactant for the main part of this study, since previous studies have shown that the alkyl volume presented by double-tailed surfactants is large enough to induce liquid crystallinity [24].

II. EXPERIMENT

The complex BHC-$(C_{12}D)_6$ was prepared by 1:1 charge ratio mixing of two aqueous solutions of each component (1 mg/ml). The precipitated complex was then washed several times with water to remove residual salt. The structure of the complex is presented in Fig. 2.

Photomicrographs were taken using a ZEISS Axioplane 2 microscope with strain-free objectives and a ZEISS AxioCam camera. The phase behavior of the complex was investigated by differential scanning calorimeter (DSC). All DSC measurements were performed on a Netzsch DSC 200. The samples were examined at a scanning rate of 10 K min^{-1} by applying several heating and cooling cycles.

Small-angle x-ray scattering measurements were carried out with a Nonius rotating anode ($U=40$ kV, $I=100$ mA, $\lambda=0.154$ nm) using image plates. With the image plates placed at a distance of 40 cm from the sample, a scattering vector range of $q=0.07$–1.5 nm^{-1} was available. Two-dimensional (2D) diffraction patterns were transformed into 1D radial averages.

Wide-angle x-ray scattering (WAXS) measurements were performed using a Nonius PDS120 powder diffractometer in transmission geometry. A FR590 generator was used as the source of Cu-K_α radiation. Monochromatization of the primary beam was achieved by means of a curved Ge crystal. Scattered radiation was measured using a Nonius CPS120 position-sensitive detector. The resolution of this detector in 2θ is 0.018°. The WAXS experiments in symmetric and asymmetric reflection were carried out on a Bruker D8 instrument with Cu-K_α radiation, using Goebel mirrors and scintillation counter as detector. In this setup the sample is fixed horizontally and the x-ray tube and detector moved.

Information about optical anisotropy in aligned samples was obtained applying a transmission null ellipsometry [25]. Using this technique one can exactly estimate only in-plane $(n_x-n_y)d$ and out-of-plane $(n_x-n_z)d$ retardation in the film. Measuring separately thickness of the film (sample) and one refractive index (n_x or n_y) of oriented film we were able to find principal refractive indices of a film.

The thickness of an investigated film was determined by measuring a scratch profile with AFM ("SMENA" Scanning Probe Microscope, NT-MDT, Russia). The thickness of a cell was determined by measuring and modeling interference visible spectrum of the sample in parts without material (air gap). The visible spectra were measured with a Lambda 2 UV-Visible spectrometer (Perkin Elmer).

The refractive index measurements were done with Carl Zeiss Abbe-refractometer. The UV polarized spectra were measured with a Lambda 19 UV-Visible spectrometer (Perkin Elmer) equipped with Glan-Thompson polarizer, driven by computer-controlled stepper motors. A special custom-built sample holder was used to tilt the sample.

The IR spectra were measured with Mattson PS-10000 FTIR spectrometer. Polarized spectra were measured by placing KRS-5 wire grid polarizer (Specac, England) in the incident light path in the sample chamber. A special custom-built sample holder was used to tilt the sample.

III. RESULTS AND DISCUSSION

A. Phase characterization

The BHC-$(C_{12}D)_6$ complex material shows fan-shaped textures under crossed polarizers when pressed between two glass slides at room temperature [see Fig. 3(a)]. More rare in some parts of the sample, the complex shows Schlieren and marbled textures (probably due to some alignment effects

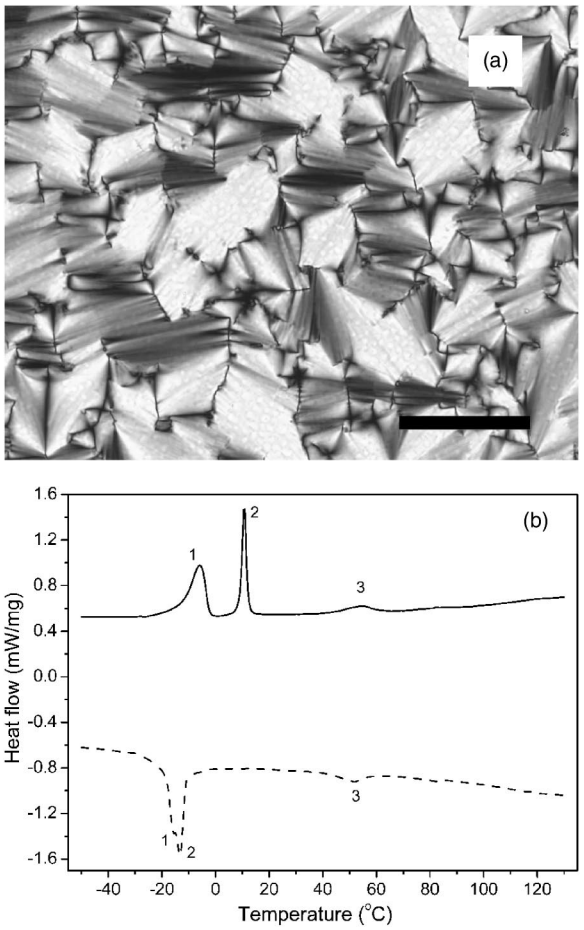

FIG. 3. (a) The fan-shaped texture of the BHC-$(C_{12}D)_6$ complex at 25 °C as observed in polarized microscope (crossed polarizers, bar: 100 μm). (b) DSC curves of the complex: second cooling circle (dashed curve) and third heating circle (solid curve).

from the preparation procedure). From the observed textures we already can make some cautious prediction that the complex exists in a smectic, most probably *A*, phase [26]. On heating to temperatures higher than 50 °C all the textures disappear. On the following cooling and heating cycles the sample appears isotropic when observed under crossed polarizers. As will be shown below, this was rather due to homeotropic alignment of the material than the absence of anisotropy. The effect of alignment will be considered in the next section. When the complex is heated to temperatures higher then 140 °C it starts to produce fine gas bubbles. This is not a result of decomposition, since thermogravimetric analysis measurements revealed decomposition temperature of the complex of approximately 170 °C. This is attributed to evaporation of water trapped in the complex, and does not affect the alignment of the material in any way (even after annealing at 150 °C).

The DSC investigations showed several transition peaks [see Fig. 3(b)]. All peaks are attributed to transitions of the surfactant alkyl chains ($C_{12}D$). Similar transitions were observed for the noncomplexed surfactant. The most prominent peaks in the range of 20 to −20 °C corresponds to crystallization of the surfactant alkyl chains. Below this temperature

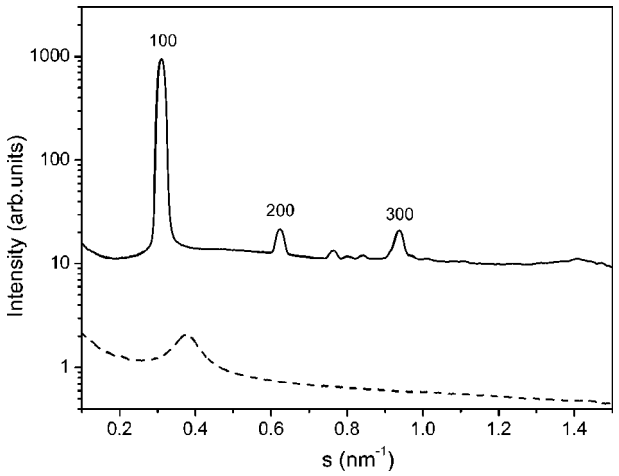

FIG. 4. SAXS diffractograms (in transmission mode) of the complex recorded at 25 °C (solid curve) and at 120 °C (dashed curve).

range the complex is crystalline. Detailed descriptions of all transitions will be given below in the part dealing with the temperature-dependent IR spectroscopy investigations.

Temperature-dependent x-ray scattering measurements were performed on annealed complex material in order to identify the LC phases present. WAXS diffractograms measured at 25 °C showed a broad peak around $2\theta = 20°$ similar to that shown by nematic and smectic-*A* mesophases [27]. This peak is attributed to a noncrystalline arrangement of the surfactant alkyl chains with an average interchain distance of 0.44 nm. The small-angle x-ray scattering (SAXS) diffractogram recorded at this temperature (Fig. 4) indicated the presence of long-range order on the nanometer scale. The three equidistant reflections correspond to a lamellar structure with a repeat distance $d_0 = 3.22$ nm. The small set of reflections noticed at higher scattering vectors ($s = 0.765$, 0.8, and 0.84 nm^{-1}) are probably due to some low correlation/internal order originating from the in-plane packing of the BHC molecules. According to generally accepted notation [28] the present phase is labeled as bilayer smectic-*A* phase (Sm-A_2).

From the SAXS diffractogram measured at 120 °C (see Fig. 4) no specific phase assignment can be made. However, it shows that the material still possesses some order on the nanometer scale. Additional proof of the proposed packing of the different fragments within the complex (at different temperatures) will be presented in the following sections.

B. Alignment properties

As was briefly mentioned in the previous section, the complex shows strong tendency to orient between two glass or quartz slides. Aligned samples were prepared by pressing the complex between two slides at 100 °C with subsequent slow cooling to room temperature. Glass powder spacers (1–90 μm) were used to control the thickness of the films. Thin films were prepared by casting of the solution of the complex in chloroform (50 mg/ml) and keeping it at room temperature under quiescent conditions to ensure very slow

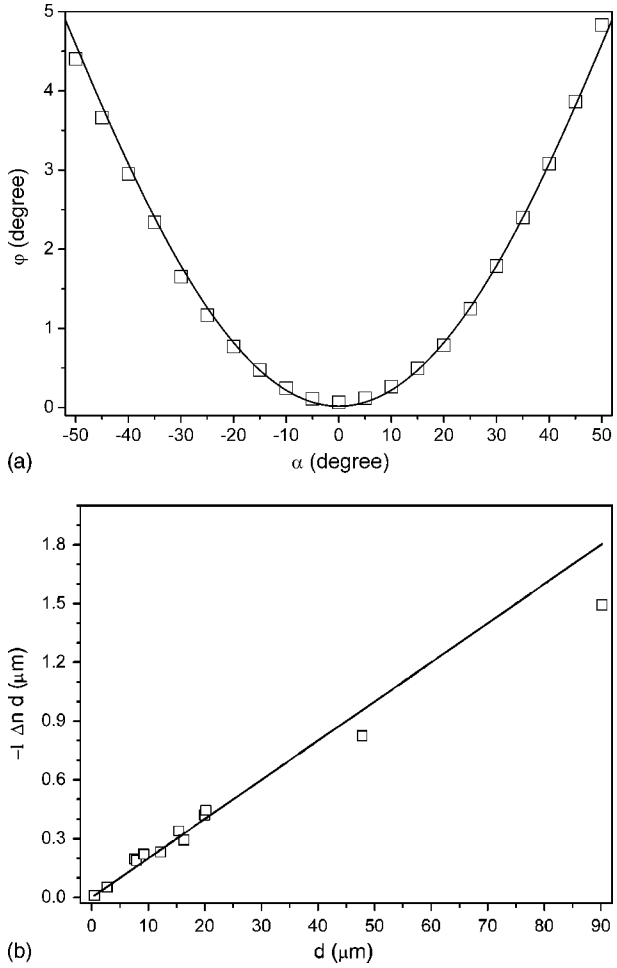

FIG. 5. (a) Experimental (□) and theoretical (—) dependences of change of the angle of polarization after quarter wave plate on tilt angle α of the sample; (b) dependence of the retardation on thickness of aligned samples.

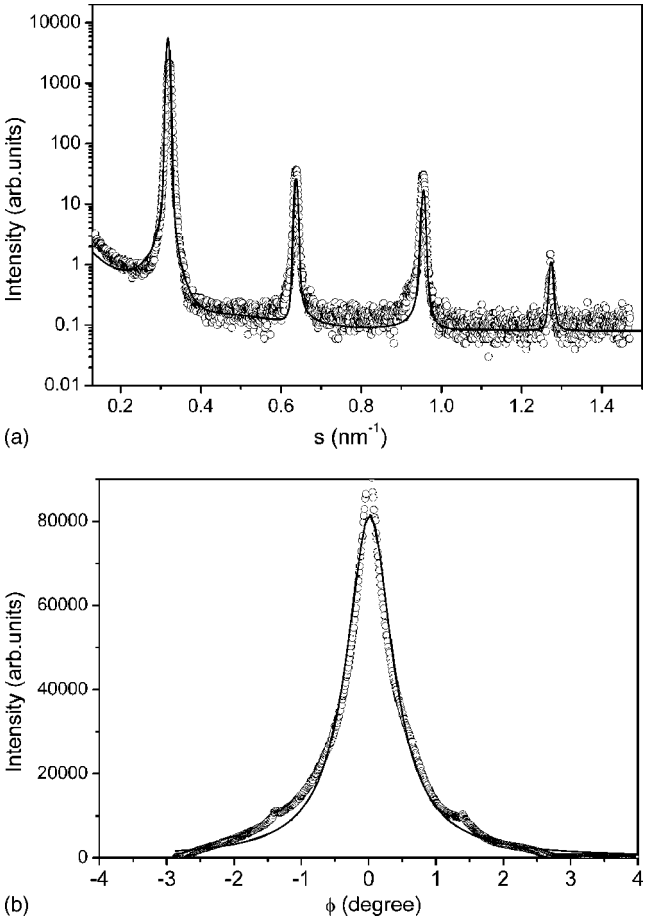

FIG. 6. (a) Measured (○) and modeled (—) small-angle x-ray reflectivity on aligned sample of the complex at 25 °C; (b) x-ray measurement in asymmetric reflection on the (001) reflection.

evaporation of the chloroform. The films were then heated to 100 °C for 30 min with subsequent cooling. It was found that neither the chemical nature (hydrophilic or hydrophobic) nor the presence (or absence) of a second (top) glass slide had any influence on the quality of the alignment.

1. Transmission null-ellipsometry

To unambiguously determine and characterize the existence of a homeotropically oriented optical axis we made use of transmission null ellipsometry. Figure 5(a) shows the experimentally obtained and modeled dependence of change of angle of polarization φ after the quarter wave plate on the tilt α of the sample [25]. From this dependence one can determine the out-of-plane retardation Δnd in the film, which was found to be negative. Measuring and modeling the interference visible spectrum of the sample in parts without material (air gap) we were able to determine the thickness of the sample between slides. The thickness of thin films (no top slide) was determined by measuring the scratch profile with AFM. The dependence of the retardation on the thickness (in different samples) is shown in Fig. 5(b). The dependence is linear, with small deviations found for large thicknesses caused by the appearance of defects (as were also observed by polarized microscopy). The found linear dependence of retardation on the thickness of the sample indicates that the complex is uniformly aligned throughout the sample (see also below).

From the slope of the curve in Fig. 5(b) we determined the difference between refractive indexes $\Delta n = -0.02$. The ordinary refractive index of the film of aligned complex was measured with an Abbe refractometer (utilizing *s*-polarized light of a He-Ne laser) and found to be $n_o = 1.490$. The extraordinary refractive index was calculated to be $n_e = 1.470$. These values were determined for $\lambda = 632.8$ nm.

2. SAXS in reflection mode

SAXS was performed in symmetric and asymmetric reflection on an aligned sample (thin film on a Si wafer), to investigate both the mesostructure and the orientation with respect to the substrate. It is seen [Fig. 6(a)] that the sample produces a series of distinct (001) interferences that are attributable to a layered mesostructure with a long period of $d_0 = 3.15$ nm. This is in very good agreement with the results from SAXS experiments using a transmission setup (described above). Furthermore, compared to the nonaligned

bulk sample, the interferences are significantly sharper, and even a fourth order peak is observed.

The appearance of several higher order interferences allowed for quantitative analysis in terms of a model [29] of two alternating types of layers of different electron densities ρ_1 and ρ_2, thicknesses d_1 and d_2, and their variances σ_1 and σ_2, taking into account the preferred orientation (see below), a finite instrumental resolution and the absorption correction. If the finite width of the boundaries cannot be neglected, a suitable approach is given by the function $H_z^2(s) = \exp(-2\pi d_z^2 s^2)$ [30], where d_z is the thickness of the interface boundary. The final expression to fit the data is $J(s) = kA(s)|I(s)H_z^2(s) + I_B|$ [29], where k is a scaling constant, $A(s)$ is the absorption correction, $I(s)$ is the ideal scattering from a lamellar two-phase system, and I_B the background scattering from 3D density fluctuations.

This basic model was considered appropriate for several reasons. First, the electron densities of the surfactant tails and the charged units are substantially different and can be estimated to be constant in the respective domain. Second, and more importantly, this model only needs a minimum number of parameters, which are physically meaningful. More detailed models cannot be expected to provide more structure information since the model used here already leads to an excellent fitting of the data. The experimental data could be excellently fitted over almost the whole range of scattering vectors s. We obtain $d_1 = 1.41$ nm and $d_2 = 1.74$ nm($\sigma_1 = 0.03$ nm, $\sigma_2 = 0.04$ nm), thus suggesting that the two layers are quite uniform in thickness, as indicated by the small values for σ_i. The model provides an estimate for the transition region between these two layers, which is calculated to be approximately $d_z = 0.2 - 0.3$ nm. In addition, the average height of the domains of the layer structure is estimated to be at least 100 nm. An exact value cannot be determined because of the finite resolution of the instrument used. In conclusion, from the SAXS modeling it can be inferred that a well-defined and extended layer structure, oriented parallel to the substrate, is present with a low degree of structural inhomogeneity.

In addition, SAXS experiments were carried out in "asymmetric reflection" mode. By this technique (see Ref. [29]), the degree of orientation with respect to the substrate can be determined. In essence, a fixed value of 2θ is chosen (here the first Bragg interference) and the x-ray tube and detector are moved (by the angle ϕ) around this position, thus providing the degree of preferred orientation of the layer structure [Fig. 6(b)]. It is observed that the experimental profile can be fitted to a Lorentzian profile with an integral width of only 0.8°. First, the observation of a maximum in asymmetric reflection proves the presence of an orientation with respect to the substrate. Second, the small value itself indicates a high degree of orientation, for instance compared to the order parameter S of liquid crystals. The formal application of the order parameter concept $S = 0.5\langle 3\cos^2\theta - 1\rangle$, taking into account the experimentally determined orientation distribution [Fig. 6(b)], leads to an averaged value of S close to 1. In summary, the SAXS experiments in symmetric and asymmetric reflection prove the existence of a highly ordered and oriented layer structure [31].

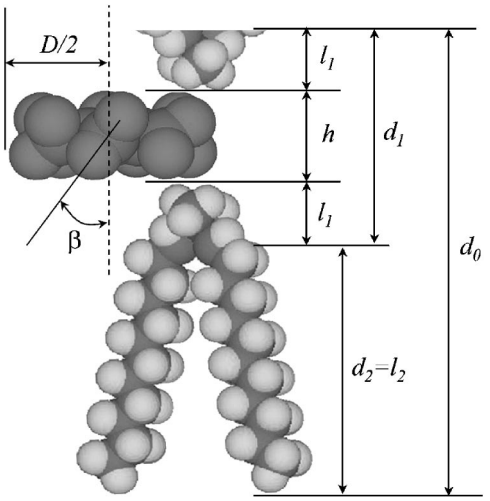

FIG. 7. Calculated molecular dimensions of the lamellar repeat unit.

In order to further verify the data obtained from the stacking model, calculations of the molecular dimensions of the molecules were performed using known lengths of the appropriate covalent bonds [32] and van der Waals radii of elements [33]. Schematic representation of BHC and $C_{12}D$ molecules with their molecular dimensions are shown in Fig. 7. For the BHC molecule we calculated the diameter $D = 0.98$ nm and height $h = 0.72$ nm. The value of the angle $\beta = 31°$ (the tilt of the carboxylate group with respect to the normal to the BHC molecule plane) used for calculations was obtained from the results of the temperature-dependent IR spectroscopy presented below. The surfactant molecule $C_{12}D$ was divided into two parts: (i) the dimethylammonium headgroup ($l_1 = 0.38$ nm) and (ii) the stretched alkyl chains ($l_2 = 1.68$ nm).

According to the x-ray model, one layer has a thickness of 1.41 nm. This would correspond very closely to the combined thickness of the benzene and headgroup sections, $d_1 = h + 2l_1 = 1.48$ nm. Full interdigitation of the alkyl layers would then fit very well with the thickness of the second layer obtained from the stacked model, with $d_2 = l_2 = 1.68$ nm. The value $d_0 = d_1 + d_2 = 3.16$ nm obtained for the d spacing from these basic calculations of the molecular dimensions is very close to that obtained from the stacked model and experimentally obtained x-ray data.

C. Ordering within the complex

To investigate the ordering of the different molecular fragments within an aligned sample we used the following techniques: angular-dependent polarized UV spectroscopy and angular-dependent polarized IR spectroscopy. In the following sections we present the results from each method. Each method gives additional useful information about the molecular packing within the layers.

1. Angular-dependent polarized UV spectroscopy

The samples for this measurement were aligned between two quartz substrates by the method described above. The

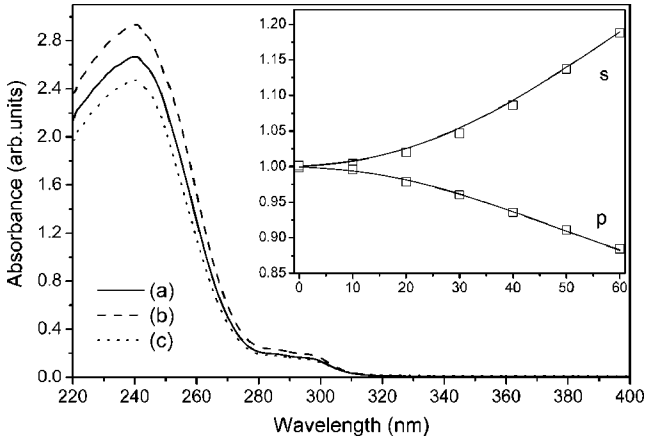

FIG. 8. Changes in polarized UV absorption spectra on tilt of the aligned sample: (a) Spectrum of aligned sample at normal incidence; (b) spectrum of *s* polarization of aligned sample at tilt angle $\alpha=60°$; (c) spectrum of *p* polarization of aligned sample at tilt angle $\alpha=60°$. Inset graph: Measured (□) and modeled (—) changes of absorbance of *s*- and *p*-polarization components at 260 nm on tilt angle α of the sample.

thickness of the sample was 2 μm and controlled with glass powder spacers. As can be seen from Fig. 8, the absorbance of the complex is characterized by two maxima in the UV range. The maxima at 290 and 240 nm correspond to the $S^1(\pi-\pi^*)$ and $S^2(\pi-\pi^*)$ transitions, respectively, of the anionic BHC molecule. The dipole moments of these transitions are parallel to the double bonds and lie in the plane of the benzene ring [34].

The polarized components of absorbance (*s* and *p*) at different angles α of incidence were measured (see Fig. 8). As a reference the same quartz substrate, as used for the preparation of the sample, positioned at the same incidence angle, was used. By using this substrate as reference the effect of reflectance of light at the air-quartz interface of the substrates could be removed. The reflectance at the interfaces between substrates and aligned complex can be neglected (as seen from the absorbance staying close to zero in the nonabsorbing part of the spectrum). There should be some reflection at these interfaces in the range of the absorbance bands, but to get qualitative results it can be neglected.

In the inset graph in Fig. 8 the dependence of normalized absorbance at 260 nm on the tilt α of the sample is shown as an example. The absorbance of *s*-polarized component increases as expected because of an increase of the optical path on the tilt of the sample. In the case of isotropic absorbance, the *s* and *p* components should increase simultaneously. However, the absorbance of the *p*-polarized component decreases dramatically. This is a result of the decrease of absorbance in the out-of-plane direction of the aligned sample. This result shows that the dipole moments of the $S^1(\pi-\pi^*)$ and $S^2(\pi-\pi^*)$ transitions of the anionic BHC molecule (and therefore also the planes of benzene rings) are aligned parallel to the substrate. Due to the dispersion of the refractive index, the negative anisotropy of the refractive index in the visible range is caused by anisotropic absorbance in the UV range. These results would therefore also fit with the proposed model (from the x-ray investigations) of the phase morphology of the complex.

To get information about the quality of ordering of the benzene rings (i.e., the order parameter), we calculated the change of absorbance on the tilt of the sample. These calculations do not consider all effects, with the main simplification being an isotropic distribution of the refractive index, but do provide qualitative results (when considering the anisotropy of the refractive index in these calculations, the calculated order parameter would have a slightly smaller value). Therefore in the case of an isotropic distribution of the refractive index the components of absorbance will be described by the formulas [35]

$$A_S(\beta) = A_X \frac{d(\beta)}{d(0)}, \tag{1a}$$

$$A_P(\beta) = [A_Y + (A_Z - A_Y)\sin^2\beta]\frac{d(\beta)}{d(0)}, \tag{1b}$$

where $d(\beta)/d(0)=1/\cos\beta$ considers changes of optical path on tilt of the sample; β is the angle between the electric field vector and the sample plane and is equal to the angle of refraction of the beam described by Snell's law: $\sin\alpha = n\sin\beta$. A_X and A_Y are components of absorbance in the plane of the sample. A_Z is the absorbance normal to the sample.

From the change in the *s*-polarized component of absorbance we determined the ordinary refractive index of the sample and used it for calculation of the *p* component of absorbance. These calculations were performed for changes of absorbance in the range 240–290 nm with steps of 10 nm. For all wavelengths the final results are similar. As an example the modeled curves at 260 nm are shown in the insert graph in Fig. 8. On the basis of these calculations the dichroic ratio $D=A_Z/A_X=0.12\pm0.01$ and corresponding spectroscopic order parameter of benzene rings (transition dipoles) $S'=(D-1)/(D+2)=-0.42\pm0.01$ were obtained. The negative value of the order parameter indicates that the dipole moments of the electronic transitions in the UV range are preferentially oriented perpendicular to the director. The director is determined, similarly to discotic LCs, as the preferential orientation of the normals to the benzene ring planes. There is a simple correlation between the order parameter of normals to the disc planes and order parameter of dipoles that are in the plane of the discs. The order parameter of normals is $S=0.5\langle 3\cos^2\theta-1\rangle$. The corresponding order parameter of the transition dipoles, which are perpendicular to the normals is $S'=0.5\langle 3\cos^2(90°-\theta)-1\rangle$. The order parameter of the normals can be obtained from the order parameter of the transition dipoles: $S=0.5-S'=0.92\pm0.01$. From this value we can conclude with certainty that the benzene rings are highly ordered.

2. Angular-dependent polarized IR spectroscopy

IR vibrational spectroscopy is a powerful tool for investigation of the ordering of liquid-crystalline systems. It was successfully applied to study the ordering of discotic LCs. The same procedure (as for UV spectroscopy) was applied for the IR spectral range. T. S. Perova *et al.* describe this method in detail in a recent review article [35]. The main

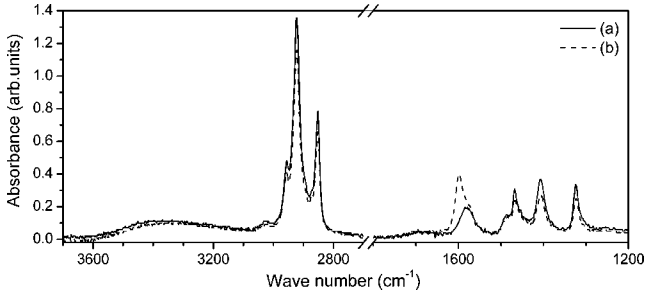

FIG. 9. Changes in polarized IR absorption spectra on tilt of aligned sample: (a) Spectrum of *s* polarization of aligned sample at tilt angle $\alpha=50°$; (b) spectrum of *p* polarization of aligned sample at tilt angle $\alpha=50°$.

difference between the IR and UV measurements is that the absorbance in the IR range is one to two orders of magnitude lower than in the UV range. The anisotropic dispersion of refractive index can therefore be reasonably neglected in the modeling, giving more accurate values of the order parameter.

To get information about the orientation of the different fragments in an aligned sample of the complex we prepared samples between two CaF_2 slides in exactly the same way as was done for the UV spectra (see above). The measurements were performed at 25 °C.

The sample thickness was determined to be 2.7 μm. This sample was also investigated with transmission null ellipsometry, and a negative homeotropically oriented optical axis with the same parameters as between two glass slides was found. Changes in the IR absorbance spectra of *s*- and *p*-polarized components on tilt of the sample are shown in Fig. 9. All bands that appear in the spectra are summarized in Table I and identified [36–38]. The band at 721 cm^{-1} is not presented in these measurements (due to the absorbance of the CaF_2 slides below 1000 cm^{-1}), but will be discussed in the section on temperature-dependent IR spectroscopy.

TABLE I. Assignment of vibrations found in IR spectra.

ν (cm^{-1})	Vibration	Tecton
721	CH_2 (ρ)	$C_{12}D$
1260	CH_2 (τ,ω)	$C_{12}D$
1323	CO_2^- (δ_s)	BHC
1375	CH_3 (δ_s)	$C_{12}D$
1409	CO_2^- (ν_s)	BHC
1466	CH_2 (δ_s)	$C_{12}D$
1485	CH_3 (δ_{as})	$C_{12}D$
1584	CO_2^- (ν_{as})	BHC
1597	CO_2^- (ν_{as})	BHC
1690	H_2O (δ_s)	water
2852	CH_2 (ν_s)	$C_{12}D$
2872	CH_3 (ν_s)	$C_{12}D$
2922	CH_2 (ν_{as})	$C_{12}D$
2954	CH_3 (ν_{as})	$C_{12}D$
3030	H_2O (ν_s)	water
3370	H_2O (ν_{as})	water

The first group of major importance corresponds to transitions of the CH_2 groups (1466, 2852, 2922). These transitions have an anisotropic distribution with a preference in the plane of the sample, as can be seen from relative value of change of the *s* and *p* absorbance components on tilt of the sample. According to the procedure described for the UV measurements we estimated the spectroscopic order parameter for each transition to be $S'(1466)=-0.20\pm0.02$, $S'(2852)=-0.25\pm0.02$, and $S'(2922)=-0.25\pm0.02$. Due to overlap with other vibrations at 1466 cm^{-1}, the resulting value of the order parameter at this frequency is lower (see Fig. 9), and we will therefore not consider it in our analyses. Taking into account that transition moments corresponding to these vibrations lie in the plane of the CH_2 group, and that this plane is perpendicular to the alkyl chains, we can conclude that the alkyl chains are aligned perpendicular to the substrates with an order parameter $S=0.5-S'=0.75\pm0.02$.

The second group of vibration frequencies of major importance originates from transitions of the CO_2^- group (1323, 1409, 1584, 1597, from the benzenehexacarboxylic acid tecton). Since the BHC molecule is completely symmetric no absorption bands corresponding to vibrations of the C=C is found. The ordering of the BHC molecules can be investigated from the CO_2^- vibrations only.

One should expect the presence of carboxylic acid dimers due to strong hydrogen bonding. Carboxylic acid dimers display very broad and intense O-H stretching absorption in the region of $3300-2500$ cm^{-1} [36]. As can be seen from Fig. 9 this band is practically absent in the IR spectrum of the complex. Instead the presence of bands corresponding to the carboxylate anion CO_2^- is observed. This is an additional proof of the formation of an one-to-one charge ratio complex.

The transition moments of the scissoring (1323) and symmetrical stretching (1409) vibrations of the carboxylate anion are in the plane of the benzene ring. Similar to UV measurements, a decrease of the *p* component of absorption is found for this band. The calculated spectroscopic order parameters for these transitions are $S'(1323)=-0.34\pm0.02$ and $S'(1409)=-0.34\pm0.02$. Again determining the director perpendicular to the plane of BHC molecules we can easily calculate the order parameter of the normals $S=0.5-S'=0.84\pm0.02$. These results are in reasonable agreement with estimations of the order parameter from angular-dependent polarized UV spectroscopy measurements. The value of the order parameter calculated from IR spectra is more realistic because, as was mentioned above, the assumption of an isotropic distribution of refractive index does not give quantitative results in the UV range.

The band at 1584 cm^{-1} corresponds to the asymmetrical stretching of the CO_2^- group. The transition moment can be, on average, at any angle to the plane of the benzene ring. This tilt may add a nonpredictable influence to the changes of absorbance of this band during tilting of the sample. In addition, this band overlaps with another band (1597 cm^{-1}) for the *p* component of absorbance on tilt of the sample, and therefore no estimation of the order parameter from changes of this band were made. The band at 1597 cm^{-1} is assigned

to the antisymmetric (out-of-phase) mechanically coupled asymmetric stretching vibration of CO_2^- group [37]. The transition moment of this vibration is perpendicular to the plane of the BHC molecule (that is, the plane of the benzene ring) and is not observed at normal incidence. This peak appears only on the tilt of the sample for the *p* component of absorbance. These changes are clearly seen in Fig. 9.

Based on all the above observations and results we can present the liquid-crystalline phase of the BHC-$(C_{12}D)_6$ complex with details of the ordering of the different molecular fragments. At room temperature the complex exhibits a layered liquid-crystalline phase (Sm-A_2). Each layer consists of a negatively charged sublayer of BHC molecules sandwiched between two sublayers of the $C_{12}D$ surfactants, compensating the negative charges. Within the negatively charged sublayer the BHC molecules are aligned with the plane of the molecules (planes of benzene rings) parallel to the surface with an order parameter of $S=0.84\pm0.02$. Within the sublayer of the $C_{12}D$ surfactant the alkyl tails are aligned perpendicular to the BHC layer with an order parameter of $S=0.75\pm0.02$. Considering that each "molecule" of the complex consists of a BHC^{6-} anion and six $C^{12}D^+$ cationic surfactants, on average three cationic surfactants can be found on each side of the anion. This aggregate can be considered as a "mesogen", and exhibits very similar molecular packing as recently found for other hexa-anionic ISA materials [39].

D. Ordering within the complex at different temperatures

To obtain further information about the temperature dependence of the order within these complexes we performed temperature-dependent IR spectroscopy measurements. The theoretical background of this method (Neff's method) is given in Ref. [35]. To show how the method can be applied to our particular system we give some conclusions from its theory. The LC sample is assumed to be aligned with the director normal to the substrates. The dichroic ratio for an unpolarized beam is defined as follows:

$$R = I_F/I_I, \tag{2}$$

where I_F is the integrated absorbance of the band in LC phase, and I_I is the integrated absorbance in the isotropic phase. Because of broadening of the bands on heating of the sample the integrated absorbance should be used instead of peak intensity. In general, the transition dipole moment of a vibration can be at angle β to the symmetry axis of molecule. The average direction of the symmetry axes of all molecules defines the director of the liquid-crystalline phase. For two particular cases of the orientation of the transition dipole moments, the order parameter can be calculated from the change of dichroic ratio:

$$S = 1 - R \ (\text{for } \beta = 0°), \tag{3a}$$

$$S = 2(R - 1)(\text{for } \beta = 90°). \tag{3b}$$

Aligned samples for these measurements were prepared between two ZnSe slides. The samples were tested with transmission null ellipsometry to show a negative homeotropically oriented optical axis with the same parameters as between two glass slides. Spectra in the range 2500–4000 cm^{-1} were measured on thin sample (thickness of 2.4 μm). Spectra in the range 650–2500 cm^{-1} were measured on thicker samples (thickness 7.5 μm, to ensure high enough absorbance for reproducible results). Temperature control of the samples was achieved within ±0.1 °C. The heating and cooling rate was 0.1° C/min. Spectra were collected in the temperature range −45–130 °C in 5 °C steps. Temperature-dependent changes of the IR spectra (at two temperatures) are presented in Fig. 10. One further band, the rocking vibration of the CH_2 group near 721 cm^{-1}, was also used (see Table I).

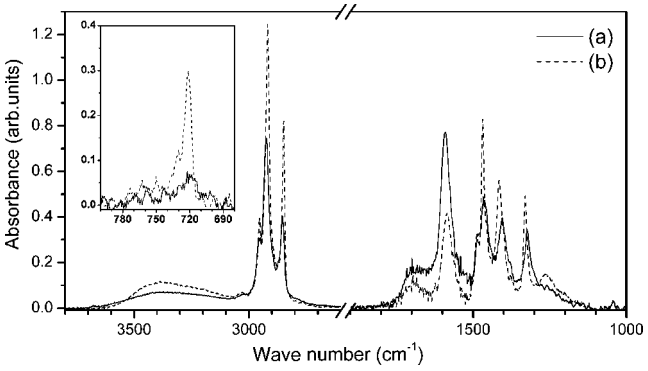

FIG. 10. Changes in IR absorption spectra of aligned sample of the complex at different temperatures: (a) 120 °C; (b) −40 °C.

All spectra were smoothed, and baseline corrections made. PEAKFIT software was used to find the peak position, to fit peaks to the sum of the Lorentzian and Gaussian functions, and to calculate the integrated areas under the peaks. The integrated intensities of some peaks were used to calculate the dichroic ratio and corresponding order parameter of the alkyl chains and benzene rings. In these calculations we encountered a problem in that we could not be sure that all the fragments of the complex were in an isotropic state at high temperature (see also the Fig. 4, SAXS diffractogram recorded at 120 °C). To overcome this problem and to find the integrated absorbance in the isotropic phase we performed the reverse calculations. From angular-dependent polarized IR spectroscopy we obtained order parameters at 25 °C. We used these values to determine the dichroic ratio from Eq. (3a) or Eq. (3b), and then using Eq. (2) we were able to obtain the integrated absorbance in the isotropic phase for an appropriate band. The obtained values we used for further calculations of temperature-dependent order parameters of appropriate fragments.

The calculated order parameter of alkyl chains from absorbance changes of the asymmetrical and symmetrical stretching vibrations of the CH_2 group is presented in Fig. 11(a). The alkyl chains are still ordered at high temperatures, as can be seen from the order parameter which reaches a plateau (0.4) and does not show any tendency to decrease with increasing temperature. At low temperatures the alkyl chains crystallize and we may expect the order parameter in the range of or very close to 1. However, the order parameter is only about 0.89 ± 0.03, clearly indicating that crystallization is restricted. These restrictions are probably due to the influence of the ionic interactions in the complex and the

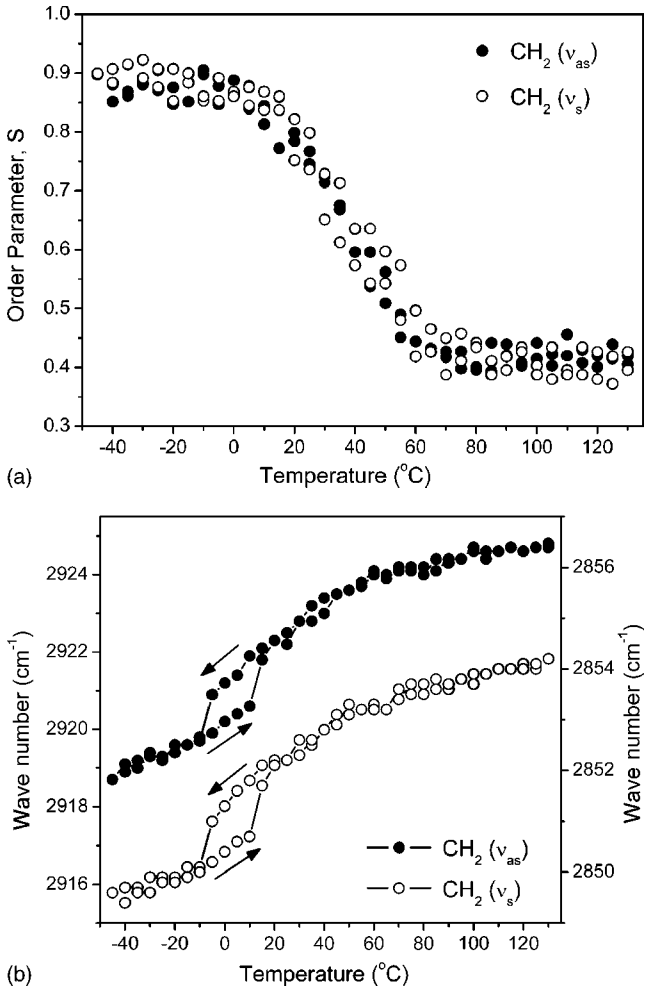

FIG. 11. (a) Calculated changes of temperature dependent order parameter of alkyl chains from absorbance changes of asymmetrical and symmetrical stretching vibrations of CH_2 group; (b) appropriate frequency shift for these vibrations on cooling-heating circle (left axes: ν_{as}; right axes: ν_s).

restrictions they impose on the organization and packing (as compared to pure covalent materials) of the long alkyl tails. The changes in order parameter are strongly correlated to the crystallization (packing) process. This can be seen from temperature changes of the normalized integrated absorbance of the in-plane CH_2 bending (rocking) vibration (Fig. 12), which acts as indicator of the crystallization (packing) behavior of the alkyl chains. Here we should also note that the transition marked with **1** in DSC curves [Fig. 3(b)] is attributed to crystallization of alkyl chains.

The frequency shifts for the CH_2 asymmetrical and symmetrical stretching vibrations are presented in Fig. 11(b). An abrupt change in frequency is found in the heating cycle at 10 °C, with an hysteresis of 20 °C in the cooling cycle. Abrupt changes in frequency and hysteresis was also observed for scissoring vibration of CH_2 group. These changes are attributed to changes in the packing of the alkyl chains with the onset of crystallization processes/events. A similar hysteresis is observed in DCS curves [Fig. 3(b)] for transition peaks marked with **2**.

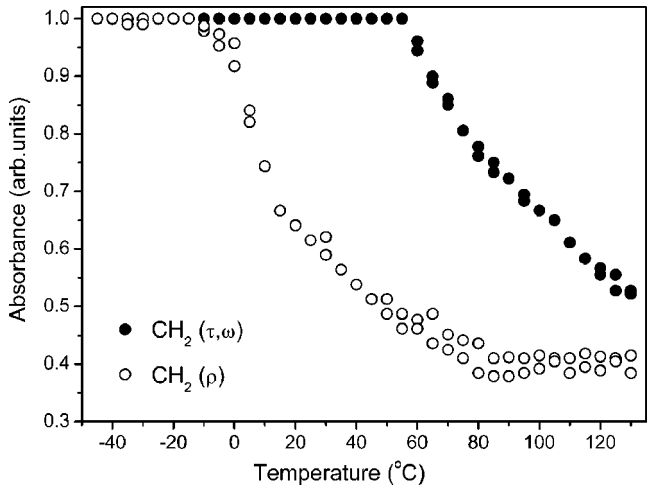

FIG. 12. Temperature changes of normalized integrated absorbance of out-of-plane bending (τ, ω) and in-plane bending (ρ) vibrations of CH_2 group.

Changes in the integrated absorbance of the out-of-plane CH_2 bending (τ, ω) vibration are connected to the "melting" process of alkyl tails (see Fig. 12). The peaks marked with **3** on DSC curves [Fig. 3(b)] are attributed to the melting of alkyl chains and correspond to the observed change. One should expect the transition to the isotropic phase to be connected with the onset of melting of the alkyl chains. However, the order parameter of the alkyl chains remains constant (0.4), which may indicate that the chains are held in their positions by the ionic interactions found within the complex.

The calculated order parameter of the BHC molecules from absorbance changes of symmetrical and asymmetrical stretching vibrations of CO_2^- group is presented in Fig. 13(a). The order parameter calculated from symmetrical vibration represents the real ordering of the benzene rings because the transition dipole of the symmetrical vibration lies in the plane of the benzene ring (i.e., it forms an angle $\beta = 90°$ with the normal of the benzene ring plane). As was already mentioned, the transition dipole of the asymmetrical vibration may form a certain angle β with the normal of the benzene ring plane. The order parameter is calculated from an assumption that this angle $\beta = 0°$ [see Fig. 13(a)]. The lower values of the order parameter are caused by this angle. If the transition dipole forms an angle β with the axis of the molecule, the order parameter should be calculated from the formula [40].

$$S = \frac{S_O}{1 - \frac{3}{2}\sin\langle\beta\rangle}, \tag{4}$$

where S_O is the order parameter calculated with the assumption that $\beta = 0°$, and S is the real order parameter. We therefore have values of the order parameter and we can calculate the average angle $\langle\beta\rangle$ of deviation of the transition dipole of the asymmetrical vibration from the normal of the benzene ring plane. This angle is also the angle between the plane of

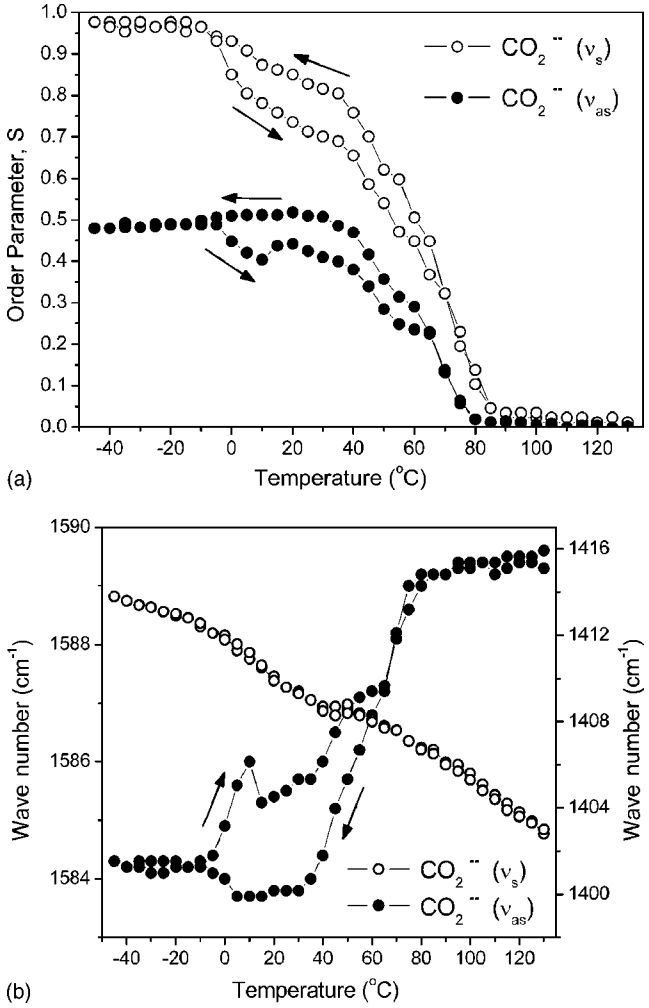

FIG. 13. (a) Calculated changes of temperature dependent order parameter of alkyl from absorbance changes of asymmetrical and symmetrical stretching vibrations of CO_2^- group; (b) and appropriate frequency shift for these vibrations on cooling-heating circle (left axes: ν_{as}; right axes: ν_s).

CO_2^- group and the normal of benzene ring plane (see Fig. 7). Calculations of this angle in the temperature range −45–−10 °C give the value $\langle\beta\rangle = 35 \pm 1°$, and in the temperature range 10–60 °C $\langle\beta\rangle = 35 \pm 1°$. Hysteresis is found at intermediate temperatures, as is also observed in DCS curves [Fig. 3(b)], exists for transition peaks marked with **2**. Calculations at elevated temperatures were not possible because of uncertainties caused by values of the order parameter being close to zero.

Hysteresis in the order parameter can be attributed to the influence of crystallization (packing) processes of the alkyl chains, which, in turn changes the position of the cationic groups. The proof that changes in the positions of the cations influence the packing of benzene rings can be seen from the frequency shift of the symmetrical and asymmetrical stretching vibrations of the CO_2^- group shown in Fig. 13(b). The transition dipole of the symmetrical vibration should not depend on the influence of the cationic layers if it is oriented in the plane of benzene ring. However, the transition dipole of the asymmetrical vibration is out of this plane at an angle $90° - \langle\beta\rangle$ and is suppressed by two layers of cations. In addition the hysteresis in the order of the benzene rings appear in the same temperature range as where the repacking process of alkyl chains take place (compare Figs. 12 and 13). We should also indicate an additional small hysteresis in the frequency of the asymmetrical vibration of the CO_2^- group [see Fig. 13(b)] in the −10–10 °C temperature range, which is connected to the re-crystallization of alkyl chains [peak **2** in Fig. 3(b)]. Finally, we note an increase of the angle $\langle\beta\rangle$ when the alkyl chains are in a crystalline state, indicating very strong immobilization of the BHC molecules within the layered structure. The ordering of the benzene tectons is strongly influenced by the packing of the alkyl chains, which are in turn strongly influenced by the presences of the (neutralized) charges. All these processes are interconnected.

An additional remarkable feature of these ISA materials is that, with a decrease in temperature, the complex crystallizes from an aligned LC phase into a single crystal domain. Practically all known low molecular LCs crystallize in multidomain structure because of thermal fluctuations. In the ISA complex the ionic interactions dominates and suppresses these fluctuations, resulting in very large monodomain structures.

E. Other complexes

We also investigated the formation of complexes with surfactants of different length and number of alkyl tails, that is, similar double-tailed ammonium surfactants ($C_{10}D$, $C_{14}D$, $C_{16}D$ ($n=m=10$, 14, 16, respectively; see Fig. 2) and the single-tail surfactant $C_{16}S$ ($n=16$, $m=1$; see Fig. 2). All these complexes show alignment behavior similar to the investigated BHC-$(C_{12}D)_6$ complex. On heating they show a strong tendency to align uniformly between two glass slides. Null ellipsometry supplemented with thickness and refractive index measurements revealed negative homeotropically oriented axes with $\Delta n = -0.020 \pm 0.003$ at $\lambda = 362.8$ nm. From this result we can predict the existence of similar layered liquid-crystalline phases in all of these complexes. Additional proof that these complexes possess similar phases is the similar optical textures observed under cross polarizers.

Similar transition peaks, which were observed for the BHC-$(C_{12}D)_6$ complex, were also observed for all other complexes in their DSC curves. The shift of the phase-transition temperatures on change of the length and structure of the surfactants is shown in Fig. 14. An increase in the phase-transition temperatures with an increase of the length of alkyl chains is clearly observed. From this dependence we can conclude that there is an opportunity, for example, to obtain a single-crystal aligned sample at room temperature just by increase of the length of the alkyl tails of the surfactant.

IV. CONCLUSIONS

We have investigated the influence of ionic interactions on the formation of LC phases in ISA complexes using the simple BHC-$(C_{12}D)_6$ complex as model system. This com-

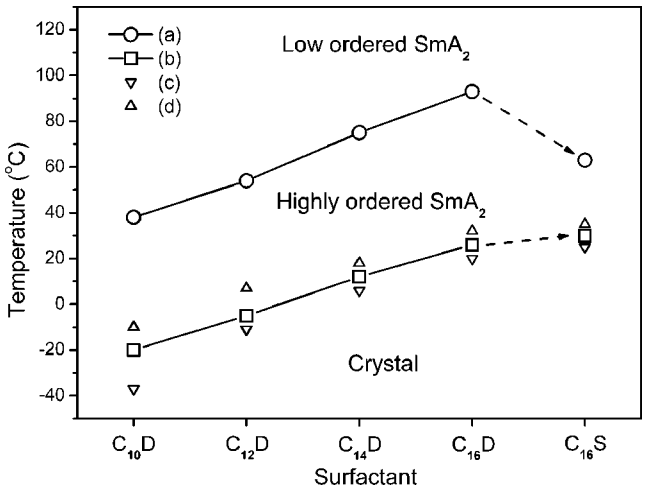

FIG. 14. Phase transition shifts of the BHC based complexes on change of the length and structure of the surfactants: (a) corresponds to peak 3 in Fig. 3(b); (b) corresponds to peak 1 in Fig. 3(b); (c),(d) correspond to hysteresis of peak 2 in Fig. 3(b) on cooling and heating curves, respectively.

plex exhibits a bilayer smectic Sm-A_2 liquid-crystalline phase. Within the first layer the BHC molecules are ordered with their planes parallel to the layers. Within the second layer, alkyl chains are ordered perpendicular to the layers. This is in stark contrast to the usual phase behavior found for any benzene-based discotic materials, which usually form columnar phases.

The complex aligns spontaneously, with the alignment properties not depending on the nature or treatment of the slides. The aligned complex possesses a negative homeotropically oriented optical axis ($\Delta n = -0.02$ at room temperature), with layers aligned parallel to the slide surface.

Temperature-dependent IR spectroscopy measurements on the aligned complex revealed that the complex crystallize from the aligned LC phase into a single crystal domain on cooling below −10 °C. This is a remarkable feature of the ionic interactions in ISA complexes, where dominating ionic interactions suppress fluctuations appearing during the crystallization process. Practically all known low molecular weight LCs crystallize in multidomain structures because of these fluctuations. The presence of the ionic interactions also suppresses the transition to an isotropic phase. This would therefore also indicate that all other interactions, except the ionic interactions between the tectonic groups and hydrophobic interactions between the alkyl tails, can be largely neglected.

Besides the importance of such simple complexes in the basic investigations of the influence of ionic interactions on the formation of ISA complexes, these complexes may also find industrial applications. The first application of such complexes could be as negative compensation film for improvement of viewing angle of liquid-crystal displays [41,42]. Cheap in synthesis, easy in alignment, and broad retardation range depending on the film thickness (10–600 nm) are remarkable advantages of these materials. Since the SAXS diffractogram of this material shows a series of well-defined, sharp interferences, films prepared from the complexes could therefore also be envisaged as possible candidate for low-cost x-ray monochromators.

ACKNOWLEDGMENTS

We thank Carmen Remde for technical support and Professor G. Puchkovskaya (Institute of Physics of NASU, Kyiv, Ukraine) for fruitful discussions and help in the analyses of the IR spectra. Dr. Ying Guan is thanked for providing the initial materials. The MPG and FHG are gratefully acknowledged for financial support.

[1] D. Demus, in *Handbook of Liquid Crystals*, edited by D. Demus, J. Goodby, G. W. Gray, H.-W. Spiess, and V. Vill (Wiley-VCH, Weinheim, 1998), Vol. 1, Chap. VI.
[2] R. J. Bushby and O. R. Lozman, Curr. Opin. Colloid Interface Sci. **7**, 343 (2002).
[3] N. V. Madhusudana, in *Liquid Crystals. Applications and Uses*, edited by B. Bahadur (World Scientific, Singapore, 1990), Vol. 1, Chap. 2.
[4] D. Demus and A. Hauser, in *Selected Topics in Liquid Crystal Research*, edited by H.-D. Koswig (Akademie-Verlag, Berlin, 1990), p. 19.
[5] P. G. de Gennes and J. Prost, *The Physics of Liquid Crystals* (Oxford University Press, New York, 1995), Chap. 6.
[6] W. Weissflog, in *Handbook of Liquid Crystals* (Ref. [1]), Vol. 2B, Chap. XI.
[7] W. Sipula, M. Kastler, D. Wasserfallen, T. Pakula, and K. Muellen, J. Am. Chem. Soc. **126**, 8074 (2004).
[8] M. Gharbia, A. Gharbi, H. T. Nguyen, and J. Malthete, Curr. Opin. Colloid Interface Sci. **7**, 312 (2002).
[9] C. T. Imrie and P. A. Henderson, Curr. Opin. Colloid Interface Sci. **7**, 298 (2002).
[10] S. A. Hudson and P. Maitlis, Chem. Rev. (Washington, D.C.) **93**, 861 (1993).
[11] J. L. Serrano, *Metallomesogens* (Wiley-VCH, Weinheim, 1996).
[12] B. Donnio, Curr. Opin. Colloid Interface Sci. **7**, 371 (2002).
[13] V. Percec, *et al.*, Nature (London) **419**, 384 (2002).
[14] T. Kato, in *Handbook of Liquid Crystals* (Ref. [1]), Vol. 2B, Chap. XVII.
[15] T. Kato, N. Mizoshita, and K. Kanie, Macromol. Rapid Commun. **22**, 797 (2001).
[16] C. F. J. Faul and M. Antonetti, Adv. Mater. (Weinheim, Ger.) **15** (9), 673 (2003).
[17] Y. Guan, Y. Zakrevskyy, J. Stumpe, M. Antonietti, and C. F. J. Faul, Chem. Commun. (Cambridge) **2003**, 894 .
[18] Y. Zakrevskyy, C. F. J. Faul, Y. Guan, and J. Stumpe, Adv. Funct. Mater. **14**, 835 (2004).
[19] M. L. Bushey, A. Hwang, P. W. Stephens, and C. Nuckolls, J. Am. Chem. Soc. **123**, 8157 (2001).
[20] T. Q. Nguyen, M. L. Bushey, L. E. Brus, and C. Nuckolls, J.

Am. Chem. Soc. **124**, 15051 (2002).
[21] M. L. Bushey, A. Hwang, P. W. Stephens, and C. Nuckolls, Angew. Chem., Int. Ed. **41**, 2828 (2002).
[22] L. Eshdat, R. E. Hoffman, A. Fechtenkoetter, K. Muellen, and M. Rabinovitz, Chem.-Eur. J. **9**, 1844 (2003).
[23] S. Chandrasekhar, B. K. Sadishiva, and K. A. Suresh, Pramana **9** (5), 471 (1977).
[24] Y. Guan, M. Antonietti, and C. F. J. Faul, Langmuir **18**, 5939 (2002).
[25] O. V. Yaroshchuk, A. D. Kiselev, Yu. Zakrevskyy, T. Bidna, J. Kelly, L.-C. Chien, and J. Lindau, Phys. Rev. E **68**, 011803 (2003).
[26] I. Dierking, *Textures of Liquid Crystals* (Wiley-VCH, Weinheim, 2003).
[27] P. Mariani, F. Rustichelli, and G. Torquati, in *Physics of Liquid Crystalline Materials*, edited by I.-C. Khoo (OPA B. V., Amsterdam, 1991), Chap. 1.
[28] J. W. Goodby and G. W. Gray, in *Handbook of Liquid Crystals* (Ref. [1]) Vol. 1, Chap. II.
[29] W. Ruland and B. Smarsly, J. Appl. Crystallogr. **37**, 575 (2004).
[30] W. Ruland, Colloid Polym. Sci. **255**, 417 (1977).
[31] The small additional maxima around ±1.5° in this experimental setup correspond to reflections originating from the Si wafer.
[32] *CRC Handbook of Chemistry and Physics*, 80th edition (CRC Press, Boca Raton, 1999–2000), Sec. 9, pp. 1–14.
[33] D. W. Van Krevelin, *Properties of Polymers* (Elsevier, Amsterdam, 1990), Chap. 4, p. 71.
[34] J. B. Lambert, H. F. Shurvell, D. A. Lightner, and R. G. Cooks, *Introduction to Organic Spectroscopy* (Macmillan, New York, 1987), Part 3, pp. 247–312.
[35] T. S. Perova, J. K. Vij, and A. Kocot, Adv. Chem. Phys. **113**, 341 (2000).
[36] R. M. Silverstein, G. C. Bassler, and T. C. Morrill, *Spectroscopic Identification of Organic Compounds* (Wiley, New York, 1994), Chap. 3, pp. 91–164.
[37] H. F. Shurvell, in *Handbook of Vibrational Spectroscopy*, edited by J. M. Chalmers and P. R. Griffiths (Wiley, Weinheim, 2002), Vol. 3, pp. 1783–1817.
[38] J. B. Lambert, H. F. Shurvell, D. A. Lightner, and R. G. Cooks, *Introduction to Organic Spectroscopy* (Macmillan, New York, 1987), Part 2, pp. 133–239.
[39] J. Kadam, C. F. J. Faul, and U. Scherf, Chem. Mater. **16**, 3867 (2004).
[40] L. M. Blinov, *Electro-optical and Magneto-optical Properties of Liquid Crystals* (Wiley, New York, 1983), Chap. 2, p. 41.
[41] H. Mori, Y. Itoh, Y. Nishiura, T. Nakamura, and Y. Shinagawa, Jpn. J. Appl. Phys., Part 1 **36**, 143 (1997).
[42] T. Sergan, M. Sontatki, J. Kelly, and L.-C. Chien, Mol. Cryst. Liq. Cryst. Sci. Technol., Sect. A **359**, 245 (2001).